Bioelectrochemistry 123 (2018) 211–218

Contents lists available at ScienceDirect

Bioelectrochemistry

journal homepage: www.elsevier.com/locate/bioelechem

A sensitive electrochemiluminescent biosensor based on AuNP-functionalized ITO for a label-free immunoassay of C-peptide

Xiang Liu [a,1], Chen Fang [a,b,1], Jilin Yan [a], Huiling Li [c,*], Yifeng Tu [a,*]

[a] Institute of Analytical Chemistry, Dushu Lake Campus, Soochow University, Industrial Park, Suzhou 215123, PR China
[b] Second Affiliated Hospital, Soochow University, Suzhou 215004, PR China
[c] College of Nursing, First Affiliated Hospital, Soochow University, Suzhou 215006, PR China

ARTICLE INFO

Article history:
Received 14 December 2017
Received in revised form 16 May 2018
Accepted 19 May 2018
Available online 23 May 2018

Keywords:
Electrochemiluminescence
Immunosensor
Luminol
Diabetes
C-peptide

ABSTRACT

The C-peptide is a co-product of pancreatic β-cells during insulin secretion; its content in body fluid is closely related to diabetes. This paper reports an immune-sensing strategy for a simple and effective assay of C-peptide based on label-free electrochemiluminescent (ECL) signaling, with high sensitivity and specificity. The basal electrode was constructed of an indium tin oxide (ITO) glass as a conductive substrate, which was decorated by Au nanoparticles (AuNPs) with hydrolysed (3-aminopropyl)trimethoxysilane as the linker. The characteristics of the fabricated electrode were investigated by electron microscopy, cyclic voltammetry, and electrochemical impedance spectroscopy. After immobilizing the C-peptide antibody, which takes great advantage of AuNPs' binding capacity, this immunosensor can quantify C-peptide using luminol as the ECL probe. By measuring ECL inhibition, calibration can be established to report the C-peptide concentration between 0.05 ng mL^{-1} and 100 ng mL^{-1} with a detection limit of 0.0142 ng mL^{-1}. As a proof of concept, the proposed strategy is a promising and versatile platform for the clinical diagnosis, classification, and research of diabetes.

1. Introduction

C-peptide, also known as the connecting peptide, is a component of blood secreted by pancreatic cells. Human C-peptide consists of 31 amino acids with an isoelectric point of approximately pH 3.0 [1]. Because it is produced by the proteolytic dissociation of proinsulin, its amount is equimolar to that of insulin. C-peptide is barely absorbed by the kidneys, resulting in the excretion of at least 85% in urine [2]. The half-life of C-peptide in plasma (20 to 30 min) is longer than that of insulin (3 to 5 min), making it five times more concentrated than insulin [3]. Human C-peptide concentration in urine (reference interval, 40 to 150 ng mL^{-1}) [4,5] or in plasma (0.5 to 10.0 ng mL^{-1}) [6,7] can indicate the early failure of insulin secretion in the preclinical stages of diabetes. As a result, considering its constancy and persistence, the blood C-peptide content has become an important marker for diabetic patients and provides a means to distinguish type 1 and type 2 diabetes [8,9].

Several methods have been developed for C-peptide detection. Kippen et al. first reported a method for serum C-peptide measurement that utilized a solid phase extraction cartridge and immunoaffinity purification using an immobilized antibody column [6]. Others have reported chromatography-based methods such as two-step solid phase extraction and two-dimensional chromatographic methods [10,11]. Although these methods function over a wide range of serum C-peptide concentrations, their lack of sensitivity requires large amounts of serum resulting in high detection cost and sometimes reduced reliability.

The measurement of C-peptide has been routinely performed by immunoassays [2]. Immunoassay is a detection method based on specific immune recognition. It established the standard for biodetection that can be used in clinical laboratories for diagnosis, the food industry, and environmental contamination monitoring [12–17]. Compared to conventional immunoassays, electrochemical immunosensors based on highly specific immune recognition have received increasing attention due to their simple construction, lower detection limit with small sample quantities, fast procedure, ease of mass-production, and potential for miniaturization [18]. C-peptide biosensors, with their intrinsic biorecognition ability, also have benefits including high specificity, simple operation, and low cost [19].

The most crucial step in the construction of immunosensors is the immobilization of the immune component (antibody or sometimes antigen) on a solid supporting surface for target capturing [20]. Gold nanoparticles (AuNPs), one of the most widely used nanomaterials in electrochemical immunosensors, have excellent abilities for binding

* Corresponding authors.
E-mail addresses: lhl8543@126.com, (H. Li), tuyf@suda.edu.cn (Y. Tu).
[1] These authors contributed equally to this work.

https://doi.org/10.1016/j.bioelechem.2018.05.010
1567-5394/

biomolecules (such as proteins, enzymes, and antibodies) due to their unique physicochemical properties such as large surface-to-volume ratio, non-toxicity, good conductivity/catalysis, and biocompatibility [21,22]. However, controlling the size, dispersity, morphology, surface chemistry, and assembly of AuNPs on an electrode surface remains a great challenge in real-life applications [23,24]. Therefore, it is crucial to explore novel strategies, both materials and approaches, for stabilizing AuNPs in order to enhance the immobilization efficiency of biomolecules and improve the overall performance of immunosensors.

In recent years, ECL analysis has greatly progressed due to its distinct advantages such as high sensitivity, spatio-temporal controllability, simple set-up, and low background noise [25–27]. Because of its nontoxicity, low cost, and high quantum yield, luminol is one of the most widely used luminescent reagents and has been used in ECL detection for many biomarkers [28–31]. It has also already been demonstrated that ECL biosensing via an immune-strategy on nanomaterial-functionalized indium tin oxide (ITO) glass performed well in these instances [32].

In this study, the AuNPs nanomaterials were assembled on the surface of ITO via the adhesion of a hydrolysed polymer of (3-aminopropyl)trimethoxysilane (APTMS). After that the C-peptide antibody was loaded onto the surface of electrode using the AuNPs. Utilizing the inhibited ECL of luminol as sensing signal, a label-free direct ECL immunosensor was built for C-peptide detection via specific immune recognition. Its ease of operation, low cost, excellent reproducibility, and potential for industrial mass-production makes it suitable for clinical use as a disposable device for in point-of-care tests (POCTs).

2. Experiments

2.1. Reagents and materials

ITO glass was provided by Suzhou Nippon Sheet Glass Electronics Co. Ltd. (Suzhou, China) and was used as a working electrode after being cut into 1.0 cm × 5.0 cm pieces. Luminol was purchased from Fluka (Sigma-Aldrich China, Shanghai, China). C-peptide and its antibody (Anti-C-peptide, $M_W = 33$ kDa, 1 mg mL^{-1}) were obtained from Beijing Biosynthesis Biotechnology Co. Ltd. (Beijing, China). 3-Aminopropyltrimethoxysilane (APTMS), chloroauric acid ($HAuCl_4 \cdot 4H_2O$), trisodium citrate, bovine serum albumin (BSA, 96–99%), and phosphate ($NaH_2PO_4 \cdot 2H_2O$ and $Na_2HPO_4 \cdot 12H_2O$) were obtained from Sinopharm Chemical Reagent Co. Ltd. (Shanghai, China). All chemicals and reagents were of analytical grade without further purification. Phosphate buffer solution (0.2 M, pH 8.0) containing 5×10^{-8} M luminol served as the electrolyte in ECL analysis. Ultrapure water was used throughout the experiments.

2.2. Instruments

The ECL experiments were carried out on our lab-built apparatus as reported in a previous paper [33] using a three-electrode system (with a Pt wire as auxiliary electrode and Ag/AgCl as reference electrode). An RST-5200 Electrochemical Workstation (Risetest Instruments Co. Ltd., Suzhou, China) was used for electrochemical impedance spectroscopy (EIS) and cyclic voltammetry (CV) measurements. Scanning electron microscopy (SEM) (S-4700 scanning electron microanalyzer, Hitachi, Japan) was used to observe the surface morphology of AuNPs/ITO and resulting immunosensor, and transmission electron microscopy (TEM) (FEI, USA, at an accelerating voltage of 200 KV) was used to measure the form and size of the AuNPs.

2.3. AuNPs preparation

AuNPs were prepared according to a previous report [34]. Briefly, 4.5 mL of 1% sodium citrate solution was added to 100 mL of boiling 0.01% $HAuCl_4$ solution, and the reaction was allowed to proceed until the colour of the solution changed to wine red. The size of the obtained AuNPs was approximately 15 nm. Next, 4 mL of freshly prepared AuNPs sol was centrifuged at 3000 rpm for 10 min and then at 10000 rpm for 30 min. Then, the concentrate was re-dispersed with water to 250 μL and a homogeneously sized AuNPs sol was acquired.

2.4. Biosensor preparation

Prior to each experiment, a flake of ITO was ultrasonically washed sequentially with a 1:1 (v/v) ethanol/NaOH (1 M) mixture, acetone, and ultrapure water (20 min each) then immersed in 30% $NH_3 \cdot H_2O$ for 12 h to create a hydrophilic surface with dense -OH groups (first step in Scheme 1). After drying with a nitrogen flow, the APTMS solution of anhydrous ethanol (0.05%, v/v) was dropped onto the ITO flake, followed by waiting for the complete volatilization of ethanol. Then, this obtained ITO flake was placed in a wet environment at 55 °C to ensure the complete hydrolysis of APTMS (second step in Scheme 1). Subsequently, 50 μL of prepared AuNPs sol was dropped onto the ITO surface and left undisturbed for 3 h to deposit the AuNPs (third step in Scheme 1). Finally, it was rinsed with water and dried under nitrogen flow.

The anti-C-peptide had high affinity for AuNPs via electrostatic interaction, thus the resulting AuNPs/ITO electrode can provide a substrate for immobilizing the antibody with good bioactivity and stability. Then, 10 μL of anti-C-peptide solution was dropped onto the AuNPs/ITO electrode, incubated for 2 h at 30 °C (step four in Scheme 1), and blocked by BSA solution (2%) for 1 h at 25 °C to avoid non-specific binding (step five in Scheme 1). The resultant sensor was then washed with PBS (pH 7.4) to remove non-chemisorbed species. The sensor was dried under a nitrogen gas environment after every step and finally stored at 4 °C.

2.5. The formality of ECL detection

On each electrode containing the as-prepared immunosensor, the ECL emission of luminol is triggered by a pulsed voltage that induces luminol oxidation, yielding excitons that then radiate the light during de-excitation. The upper/lower limiting potentials and pulse period of the pulsed voltage, which greatly affect the ECL performance, require optimization. Under optimal conditions, the synchronized pulsed ECL signal pulse can be recorded, depending on the electrode surface status or concentration of some participant. The sensing output can then be detected by measuring the average of a cluster of pulses and quantified by correlating the response to the target concentration.

3. Results and discussion

3.1. Optimization of AuNPs functionalized ITO electrode performance

The AuNP-functionalized substrate electrode plays an important role in sensor construction. Therefore, some design parameters were optimized to obtain higher performance. Through analysis of the performance with multiple parameter values as listed in Fig. 1, we chose 10 μL of 0.05% APTMS for hydrolysis under 55 °C for 3 h and decoration with 1.93×10^{-6} mol (380 μg) of AuNPs over a 3 h time period for optimal performance.

Under those optimized conditions, 85.3% surface coverage of ITO by AuNPs was obtained. This result was determined by a cyclic voltammetric scan of the $K_3Fe(CN)_6$ probe to calculate the real active area of the electrode according to the Randles-Sevcik equation. The active area of the electrode is 1.71 times larger after AuNPs decoration. The covering of hydrolysed APTMS on ITO might hinder the electron transfer of electrode without deposited AuNPs. The weight of the spherical Au nanoparticles causes them to penetrate the thin film and to come into direct contact with the ITO, enabling electron transfer. When controlling the thickness of APTMS to less than half size of AuNPs, these results

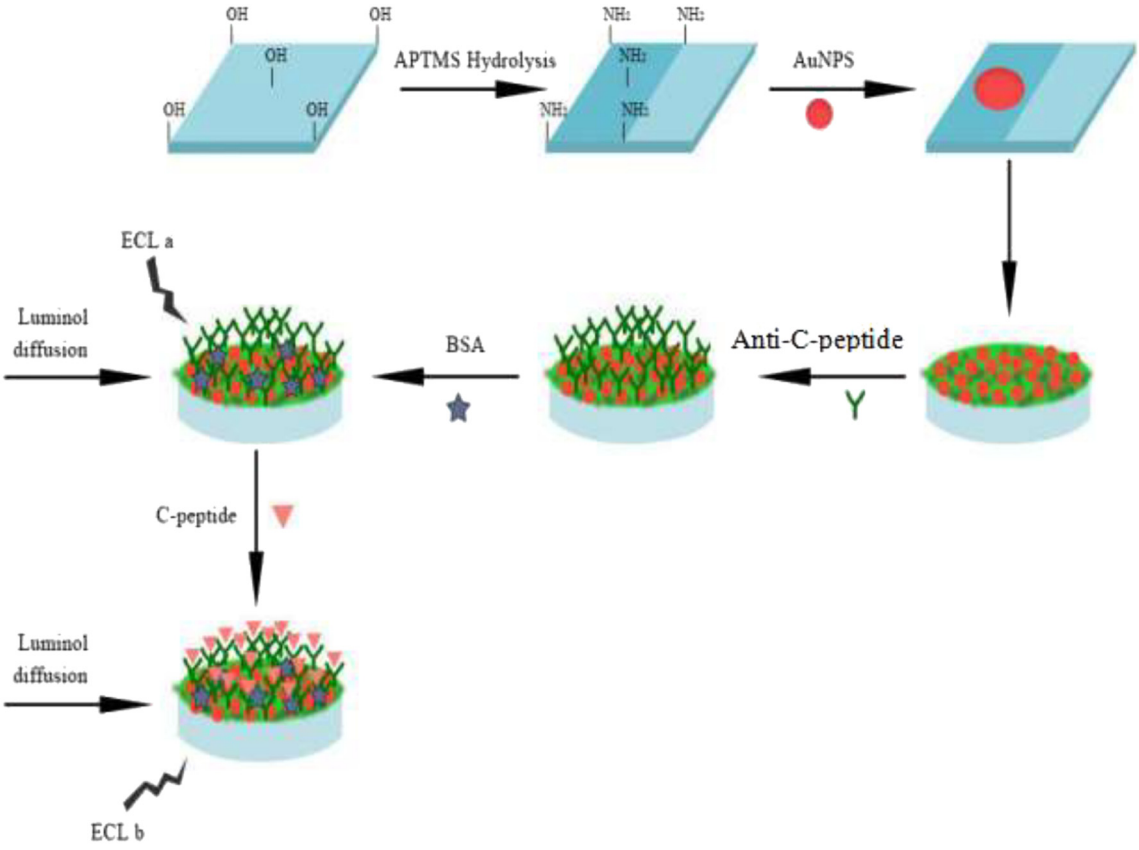

Scheme 1. The fabrication procedure and sensing mechanism of the biosensor.

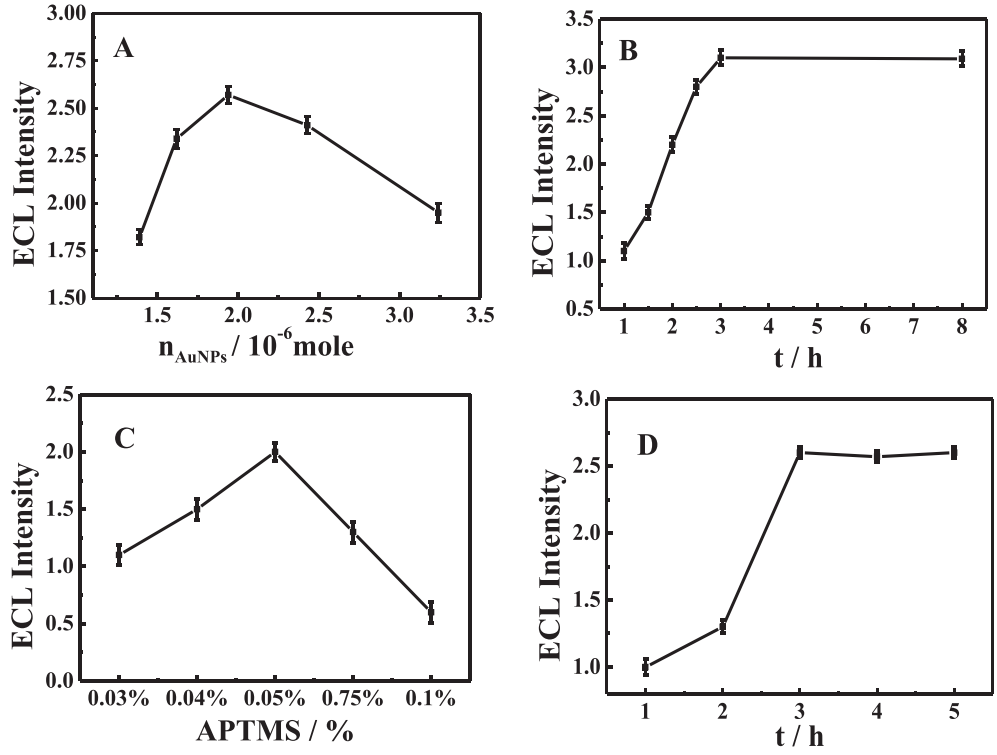

Fig. 1. The effects of control variates of (A) the amount of AuNPs (the mole number of AuNPs, $\mathbf{n}_{AuNPs}$); (B) the time for AuNPs decoration; (C) the content of APTMS and (D) the period of APTMS hydrolysis, on final performance of so-prepared sensor.

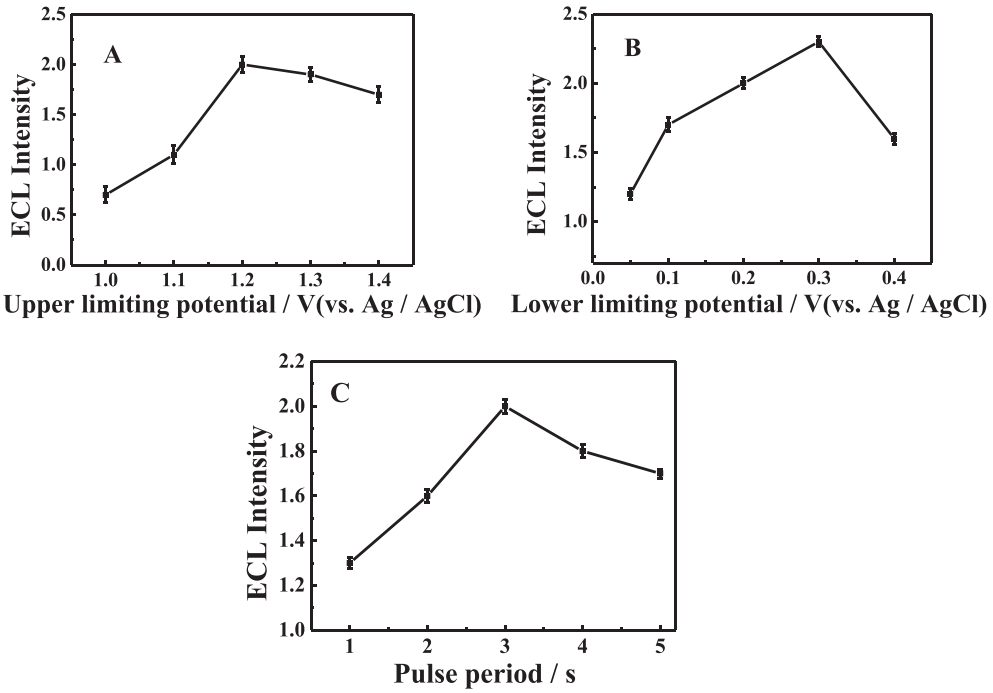

Fig. 2. The effects of (A) upper/(B) lower limiting potential and (C) pulse period of electrolytic power on the ECL emission of luminol. $C_{luminol} = 5 \times 10^{-7}$ M, pH = 8.0.

demonstrated that decoration of AuNPs on ITO is beneficial for sensor fabrication.

The upper/lower limiting potentials and the period of pulsed electrolytic voltage for ECL exciting also influence the sensor performance. As shown in Fig. 2A and Fig. 2B, setting 1.2 V as the upper and 0.3 V as the lower limiting potentials, respectively, with 3 s as the pulse period (Fig. 2C) results in the highest ECL intensity.

3.2. Optimization of immunosensor preparation and detection conditions

The performance of biosensor sensing output is dependent on the assembling of anti-C-peptide on the abovementioned substrate electrode (step 4 in Scheme 1). Anti-C-peptide assembling conditions must all be optimized including the concentration, temperature, and duration. Fig. 3A reveals that the ECL intensity decreased drastically with increasing anti-C-peptide concentration until remaining steady at 0.025 μg mL^{-1}, indicating anti-C-peptide saturation on the AuNPs/ITO electrode. The influence of temperature and immobilization time was also examined. As shown in Fig. 3B and Fig. 3C, a maximum was reached at 30 °C for 2 h. Additionally, for use in the sensing effect of C-peptide (step six in Scheme 1), Fig. 3(D, E) indicates that 1 h incubation under 30 °C was sufficient.

The sensor performance improves greatly under these optimized conditions, as shown by the electron microscopy results. Fig. 4 presents the SEM images of AuNPs/ITO (Fig. 4A) and the resultant sensor (Fig. 4B), respectively. AuNPs with a diameter of ~15 nm (as the inserted TEM image in Fig. 4A), are well-ordered on the surface of ITO through APTMS. Fig. 4B shows the morphology of the resultant immunosensing interface (anti-C-peptide/AuNPs). It can be clearly observed that the anti-C-peptide layer tightly covered on the surface of AuNPs, indicating successful conglutination of anti-C-peptide on AuNPs.

Cyclic voltammetry (CV) and electrochemical impedance spectroscopy (EIS) were both employed to validate and clarify the sensor characteristics. Fig. 5A presents the CV curves in a 0.1 M KCl solution containing 5 mM $Fe(CN)_6^{3-}$ at the scan rate of 50 $mV \cdot s^{-1}$. The bare ITO (curve a in Fig. 5A) showed two well-defined reversible redox peaks of $Fe(CN)_6^{3-}$. When APTMS was introduced onto the surface (curve b in Fig. 5A), the nonconductive macromolecules disrupted electron transfer, resulting in the reduction of peak current. The peak current (curve c in Fig. 5A) clearly improved after the deposition of AuNPs (even greater than bare ITO), validating the great function of AuNPs as an electron transfer channel for redox of $Fe(CN)_6^{3-}$. When the anti-C-peptide was immobilized on the AuNPs/ITO (curve d in Fig. 5A), the redox peak current of the probe decreased significantly. These results confirm the electrostatic repulsion of negatively charged anti-C-peptide toward $Fe(CN)_6^{3-}$. The specific interaction of C-peptide on anti-C-peptide (curve e in Fig. 5A) further enhances this action, as described in previous work [35–38].

The EIS curves (Fig. 5B) provide further insight into the impedance changes of the electrode surface in $Fe(CN)_6^{3-}$ buffer solution. As seen, compared to the ITO substrate (curve a in Fig. 5B), the electron transfer resistance (R_{et}) increased obviously with attached non-conducting hydrolysed APTMS (curve b in Fig. 5B). The AuNPs also significantly accelerate electron transfer, as seen in curve c in Fig. 5B (enlarged in inset one). The antibody and antigen could both delay the arrival of the electron to the sensing interface, leading to increased impedance (curves d, e in Fig. 5B), which clearly proved the immobilization of the biomolecules.

Fig. 5C shows that AuNPs greatly facilitated the redox reaction of luminol. In a 2.5×10^{-5} M luminol solution, AuNP-functionalized electrode (curve a) show a very clear oxidation peak of luminol emergence at approximately 0.46 V, which is not seen with the normal Au electrode (curve b). Fig. 5D presents the CVs of various electrodes in a PBS solution containing 2.5×10^{-5} M luminol. Neither bare ITO (curve a) nor APTMS/ITO (curve b) show obvious Faradaic current of luminol. The redox peak currents greatly increased when AuNPs were decorated on ITO (curve c). Two significant oxidation peaks at 0.46 V and 0.91 V, as well as a reduction peak at 0.36 V, are observed. This is in rough accordance with

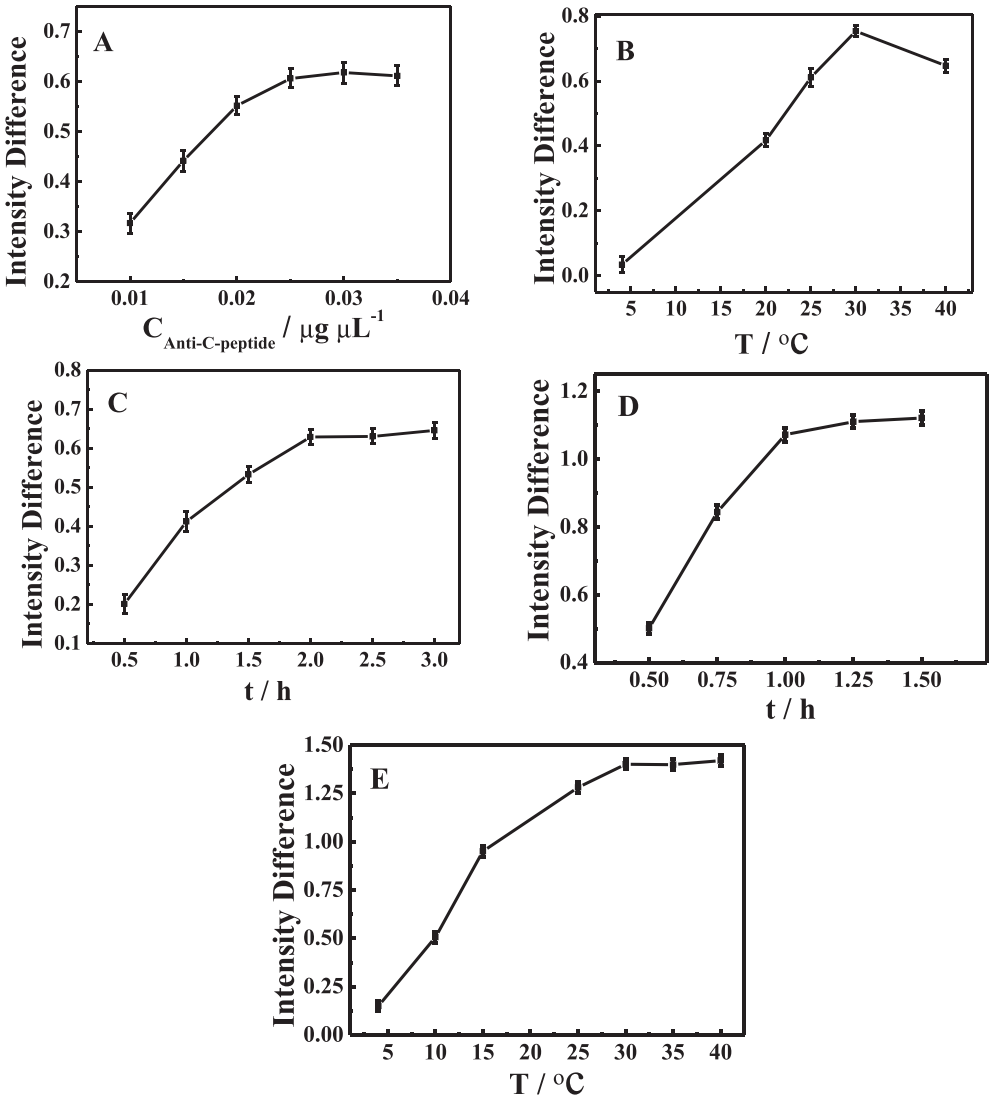

Fig. 3. The effects of (A) the anti-C-peptide concentration, (B) the temperature, (C) the incubation time for immobilization harvest of anti-C-peptide; (D) the time and (E) the temperature for C-peptide capturing on resultant sensor.

the redox behaviour of luminol on the normal Au electrode (curve d), but at a lower potential. This clearly indicates the better performance of this AuNP-functionalized electrode than the normal Au electrode for the oxidation of luminol due to the increasing d band electrons in AuNPs [39]. The decreased voltage for the redox of luminol also indicated the catalytic activity of AuNPs in reducing the activation

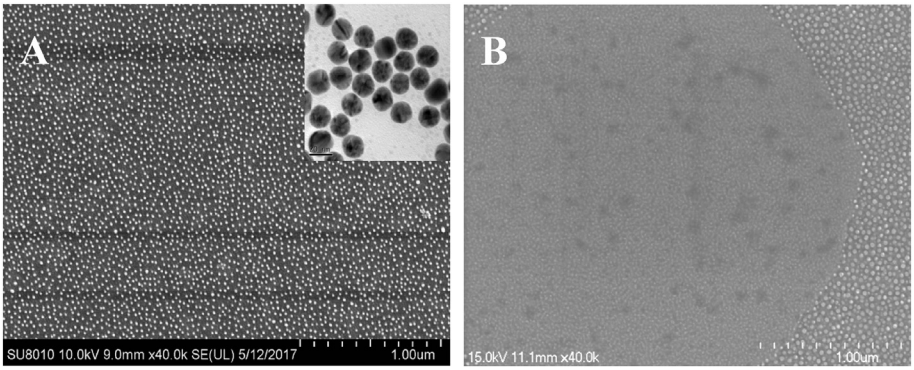

Fig. 4. The SEM images of (A) AuNPs/ITO, here the inserted one is the TEM image of AuNPs; (B) the resultant sensor (anti-C-peptide/AuNPs/ITO).

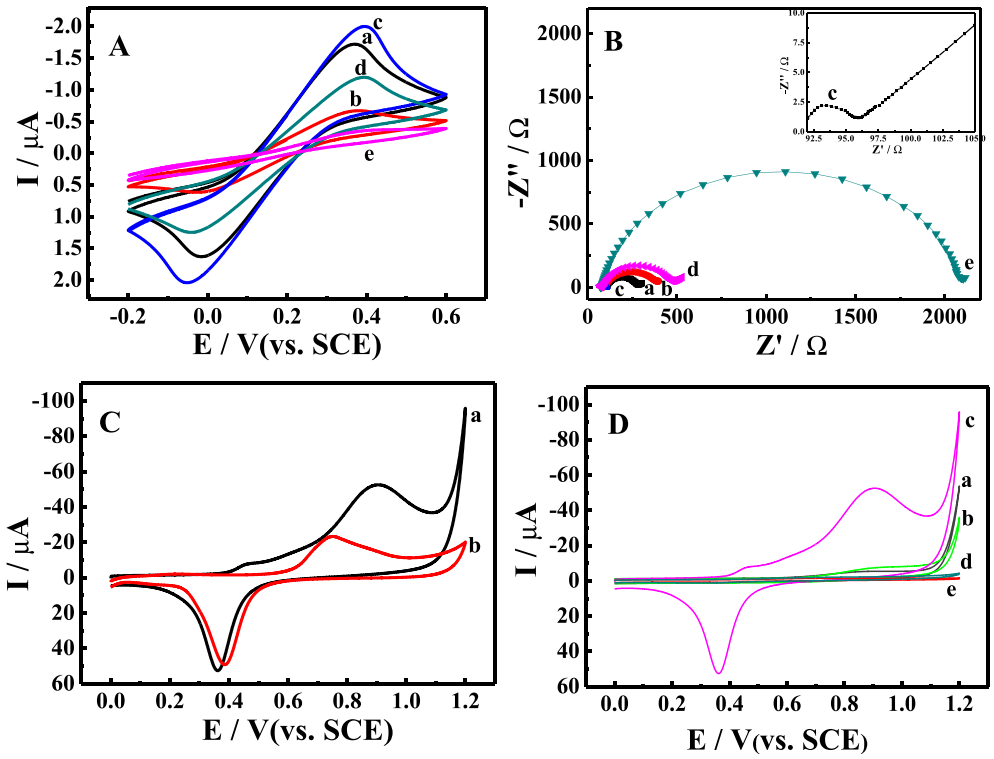

Fig. 5. (A) CV curves (at 50 mV s^{-1} of scan rate) and (B) EIS spectra (from 0.1 Hz to 100 kHz at 5 mV of AC perturbation) on (a): ITO, (b): APTMS/ITO, (c): AuNPs/ITO, (d): resultant sensor and (e): the finally responded one in 5 mM $Fe(CN)_6^{3-}$ solution. In "B", the inserted one is enlarged curve "c". (C) The comparison of redox performance of luminol on (a) AuNPs/ITO and (b) ordinary Au electrode. (D) The CV curves of luminol on (a) ITO, (b) APTMS/ITO, (c) AuNPs/ITO, (d) resultant sensor and (e) finally responded one. All in pH 8.0 PBS containing 2.5 × 10^{-5} M of luminol, under 50 mV s^{-1} of scan rate.

energy of luminol, thereby accelerating the ECL reaction. With successive deposition of C-peptide on the electrode, the peak current gradually decreased (curves e), in accordance with the EIS and ECL tests.

3.3. The sensing performance of the as-prepared sensor

Under those optimized experimental conditions, the ECL output signal or response (the difference of ECL intensity before and after the addition of C-peptide, ΔECL) on the resultant sensor with different concentrations of C-peptide was recorded. It was found that the ECL output decreased with the concentration of C-peptide (as shown in Fig. 6A). The ΔECL increased sharply with the concentration of C-peptide but gradually slowed down when the C-peptide concentration reached a certain level (as shown in Fig. 6B). The inset in Fig. 6B demonstrates that the response signals of the sensor exhibited a linear correlation to the C-peptide concentration between 0.05 ng mL^{-1} and 5 ng mL^{-1}. It can be represented by the regression equation $\Delta ECL = 0.417 + 0.585C_{C\text{-peptide}}$ ($r = 0.996$) and has a detection limit of 0.0142 ng mL^{-1} (S/N = 3, 0.142 pg of quantitative detection limit, as 10 μL of sample loading value).

As shown in Table 1, which summarizes the detection of C-peptide by other methods, it is clear that the present sensor shows remarkable sensitivity. Regardless of the method of quantification (with concentration or mass), our sensor has nearly the lowest LOD and smallest sample value.

The stability of the developed biosensor was verified using 1.5 ng mL^{-1}C-peptide under the optimized conditions. The activity of the sensor remained above 96% of its initial value after 10 days and 94% after 20 days when it was stored at 4 °C, which implies satisfactory performance.

The sensing output of the sensor was also evaluated in the presence of possible coexisting components in blood to verify whether or not those compounds would impede the detection of C-peptide. The ECL output in the presence of these compounds (10 μg mL^{-1} of uric acid (UA), 10 μg mL^{-1} of glucose, 10 μg mL^{-1} of ascorbic acid (AA), 10 μg mL^{-1} of albumin (Alb) and 15 U L^{-1} of insulin (INS)) and 1.5 ng mL^{-1} of C-peptide, as shown in Fig. 6C, demonstrates small degrees of changed ECL.

The result shown to successfully exceed the detection threshold of the normal level glucose or others in a healthy adult at a 100 times dilution of blood samples. This demonstrated that the disturbance from those coexisting compounds in blood was negligible. Thus, we can conclude that the resultant sensor performance was capable of specifically responding to C-peptide.

3.4. The applicability of the prepared sensor

To evaluate the practical use of the sensor, it was used to detect the C-peptide in the serum sample. It is difficult to evenly spread the pristine serum over the sensing surface because of its high viscosity, which can lead to a difficulty of operation and serious error. This can be a significant obstacle to real-world detection. Fortunately, with high enough sensitivity, this obstacle can be overcome by appropriate dilution, which also reduces the potential interference. We found 100- to 150-dilution was appropriate for this application. Thus, we dropped 10 μL of diluted serum on the as-prepared sensor for 1 h, and the C-peptide concentration in serum samples of two volunteers were

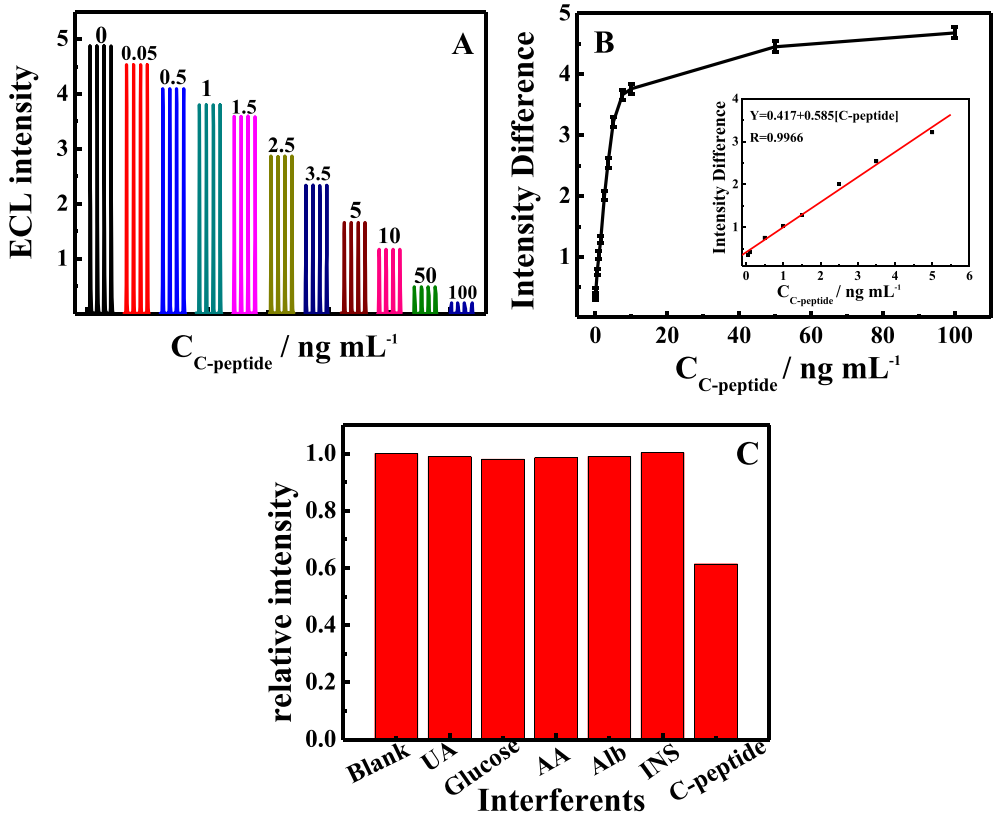

Fig. 6. (A) The real maps of ECL output on resultant sensor at differently concentrated C-peptide; (B) The dependence of responding signals on C-peptide concentrations, the inserted is its linear part from 0.05 to 5 ng mL^{-1} of C-peptide concentration; (C) The comparison of ECL output of potential coexistences toward C-peptide on resultant biosensor (1.5 ng mL^{-1} of C-peptide, 10 μg mL^{-1} of uric acid (UA), glucose, ascorbic acid (AA), albumin (Alb) and 15 U L^{-1} of insulin (INS)). The conditions are: For sensor preparation: 10 μL of 0.05% APTMS, hydrolysis under 55 °C for 3 h; 380 μg of AuNPs, depositing for 3 h; 10 μL of 0.025 μg mL^{-1} anti-C-peptide, incubated at 30 °C for 2 h; blocked by 2% BSA solution at 25 °C for 1 h. For target capturing and detection: 10 μL of sample, incubated for 1 h at 30 °C; 1.2 V and 0.3 V of upper/lower limiting potentials, 3 s of pulse period. $C_{luminol} = 5 \times 10^{-8}$ M, pH = 8.0.

determined to be 2.81 ng mL^{-1} and 3.17 ng mL^{-1}. For comparison, values of 2.9 ng mL^{-1} and 3.03 ng mL^{-1}, respectively, were obtained in our affiliated hospital. These sets of results have a 3.14% and 4.62% relative error, which demonstrate a tolerable level of detection error with our sensor. In addition, recovery tests were conducted using a standard addition method. The results ranged from 85.0% to 102%, indicating good accuracy, as shown in Table 2.

Table 1
The comparison of different methods for C-peptide determination.

Detection method	Volume of sample	Detection limit		Reference
		quality	concentration	
ID MS	35 μL	3 pg	85.7 ng L^{-1}	[2]
ID-LC	–	150 pg	–	[10]
(2D LC/MS) IDA	35 μL	300 amole (1 pg)	28.6 ng L^{-1}	[11]
LC–MS/MS	70 μL	10 pg	143 ng L^{-1}	[40]
TRFIA	150 μL	13 pg	27 pM/L (81.5 ng L^{-1})	[41]
ELISA	25 μL	2.25 pg	90 ng L^{-1}	[42]
Luminescence	–	–	83 pM/L (250 ng L^{-1})	[43]
LC	100 μL	10 μg	100 ng L^{-1}	[44]
RIA	–	–	100 ng L^{-1}	[45]
ELISA	–	–	1.5 pM/L (4.5 ng L^{-1})	[46]
TRFIA	–	–	200 ng L^{-1}	[47]
Chemiluminescent immunoassay	–	–	10 ng L^{-1}	[48]
ECL biosensor	10 μL	0.142 pg	14.2 ng L^{-1}	Present work

4. Conclusion

In this paper, a successfully prepared ECL biosensor for C-peptide via the immobilization of anti-C-peptide on AuNPs/ITO is presented. This new bioelectronic device combines the beneficial properties of nanomaterials and biocatalysts, this biosensor works in a label-free manner and requires no labelling process or external indicators, making it ideal for ECL biosensor development. With a two-step coating process, this biosensor is easily fabricated without complicated procedures or expensive instruments. Under optimal conditions, the sensor gives a detection limit of 0.0142 ng mL^{-1}, meeting the increasing need for highly sensitive, simple, reliable, reproducible, and low-cost detection for on-site monitoring.

Acknowledgements

This work is financially supported by the National Natural Science Foundation of China (21675115, 21375091).

Table 2
The detected results of C-peptide in diluted serum samples and the recoveries.

Sample no.	C-peptide in sample (ng mL^{-1})	Added (ng mL^{-1})	Found (ng mL^{-1})	Recovery (%)	RSD (%, $n = 5$)
1	1.38	1.00	2.23	85.0	3.55
2	1.62	1.50	3.05	95.2	2.98
3	2.90	2.25	5.11	98.0	2.86
4	3.03	3.50	6.12	102	2.55

References

[1] A.V. Stoyanov, C.L. Rohlfing, S. Connolly, M.L. Roberts, C.L. Nauser, R.R. Little, Use of cation exchange chromatography for human C-peptide isotope dilution-mass spectrometric assay, J. Chromatogr. A 1218 (2011) 9244–9249.

[2] T. Kinumi, R. Mizuno, A. Takatsu, Quantification of serum C-peptide by isotope- dilution liquid chromatography–tandem mass spectrometry: enhanced detection using chemical modification and immunoaffinity purification, J. Chromatogr. 953-954 (2014) 138–142.

[3] R.G. Marques, M.J. Fontaine, J. Rogers, C-Peptide: much more than a byproduct of insulin biosynthesis, Pancreas 29 (2004) 231–238.

[4] D.L. Horwitz, A.H. Rubenstein, A.I. Katz, Quantitation of human pancreatic-cell function by immunoassay of C-peptide in urine, Diabetes 26 (1977) 30–35.

[5] C. Fierens, D. Stöckl, D. Baetens, A. Leenheer, L. Thienpont, Quantitative analysis of urinary C-peptide by liquid chromatography-tandem mass spectrometry with a stable isotopically labeled internal standard, J. Chromatogr. B 792 (2003) 249–259.

[6] A. Kippen, F. Cerini, L. Vadas, R. Stocklin, L. Vu, R. Offord, et al., Development of an isotope dilution assay for precise determination of insulin, C-peptide, and proinsulin levels in non-diabetic and type 2 diabetic individuals with comparison to immunoassay, J. Biol. Chem. 272 (1997) 12513–12522.

[7] P. Clark, Assays for insulin, proinsulin(s) and C-peptide, Ann. Clin. Biochem. 36 (1999) 541–564.

[8] C. Torn, C-Peptide and autoimmune markers in diabetes, Clin. Lab. 49 (2003) 1–10.

[9] D.B. Sacks, M. Arnold, G.L. Bakris, D.E. Bruns, A.R. Horvath, M.S. Kirkman, A. Lernmark, B.E. Metzger, D.M. Nathan, Guidelines and recommendations for laboratory analysis in the diagnosis and management of diabetes mellitus, Clin. Chem. 57 (2011) E1–E47.

[10] D. Rodriguez-Cabaleiro, D. Stockl, J.M. Kaufman, T. Fiers, L.M. Thienpoint, Feasibility of standardization of serum C-peptide immunoassays with isotope-dilution liquid chromatography–tandem mass spectrometry, Clin. Chem. 52 (2006) 1193–1196.

[11] E. Rogatsky, B. Balent, G. Goswami, V. Tomuta, H. Jayatillake, G. Cruikshank, L. Vele, D.T. Stein, Sensitive quantitative analysis of C-peptide in human plasma by 2-dimensional liquid chromatography-mass spectrometry isotope-dilution assay, Clin. Chem. 52 (2006) 872–879.

[12] A.V. Stoyanov, C.L. Rohlfing, S. Connolly, M.L. Roberts, C.L. Nauser, R.R. Little, Use of cation exchange chromatography for human C-peptide isotope dilution-mass spectrometric assay, J. Chromatogr. A 1218 (2011) 9244–9249.

[13] Z.X. Zou, D. Du, J. Wang, J.N. Smith, C. Timchalk, Y.Q. Li, Y.H. Lin, Quantum dot-based immunochromatographic fluorescent biosensor for biomonitoring trichloropyridinol, a biomarker of exposure to chlorpyrifos, Anal. Chem. 82 (2010) 5125–5133.

[14] Z.H. Li, Y. Wang, J. Wang, Z.W. Tang, J.G. Pounds, Y.H. Lin, Rapid and sensitive detection of protein biomarker using a portable fluorescence biosensor based on quantum dots and a lateral flow test strip, Anal. Chem. (2010) 7008–7014.

[15] J.H. Kang, M. Korecka, J.B. Toledo, J.Q. Trojanowski, L.M. Shaw, Clinical utility and analytical challenges in measurement of cerebrospinal fluid amyloid-β1–42 and τ proteins as Alzheimer disease biomarkers, Clin. Chem. 59 (2013) 903–916.

[16] R.L. Zhang, S. Xu, J. Luo, D.J. Shi, C. Liu, X.Y. Liu, One-pot green synthesis of nanohybrid structures: gold nanoparticles in poly(γ-glutamic acid) copolymer nanoparticles, RSC Adv. (2014) 25106–25113.

[17] W.Y. Zhang, A.M. Asiri, D.L. Liu, D. Du, Y.H. Lin, Hypoxia-pretreated human MSCs attenuate acute kidney injury through enhanced angiogenic and antioxidative capacities, TrAC Trends Anal. Chem. 54 (2014) 1–10.

[18] Q. Wei, Y.F. Zhao, B. Du, D. Wu, Y.Y. Cai, K.X. Mao, H. Li, C.X. Xu, Nanoporous PtRu alloy enhanced nonenzymatic immunosensor for ultrasensitive detection of microcystin-LR, Adv. Funct. Mater. (2011) 4193–4198.

[19] S. Tang, Q. Zhao, Y.F. Tu, A sensitive electrochemiluminescent cholesterol biosensor based on Au/hollowed-TiO_2 nano-composite pre-functionalized electrode, Sensors Actuators B Chem. 237 (2016) 416–422.

[20] S. Xu, R.L. Zhang, W. Zhao, Y. Zhu, W. Wei, X.Y. Liu, J. Luo, Self-assembled polymeric nanoparticles film stabilizing gold nanoparticles as a versatile platform for ultrasensitive detection of carcino-embryonic antigen, Biosens. Bioelectron. 92 (2017) 570–576.

[21] E. Dinckaya, Ö. Kınık, M.K. Sezgintürk, Ç. Altuğ, A. Akkoca, Development of an impedimetric aflatoxin M1 biosensor based on a DNA probe and gold nanoparticles, Biosens. Bioelectron. 26 (2011) 3806–3811.

[22] B. Rezaei, N. Majidi, H. Rahmani, T. Khayamian, Electrochemical impedimetric immunosensor for insulin like growth factor-1 using specific monoclonal antibody-nanogold modified electrode, Biosens. Bioelectron. 26 (2011) 2130–2134.

[23] S. Guo, E.K. Wang, Synthesis and electrochemical applications of gold nanoparticles, Anal. Chim. Acta 598 (2007) 181–192.

[24] W. Ye, D. Wang, H. Zhang, F. Zhou, W. Liu, Electrochemical growth of flowerlike gold nanoparticles on polydopamine modified ITO glass for SERS application, Electrochim. Acta 55 (2010) 2004–2009.

[25] A. Arora, J.C.T. Eijkel, W.E. Morf, A. Manz, A wireless electrochemiluminescence detector applied to direct and indirect detection for electrophoresis on a microfabricated glass device, Anal. Chem. 73 (2001) 3282–3288.

[26] L.Z. Hu, G.B. Xu, Applications and trends in electrochemiluminescence, Chem. Soc. Rev. 39 (2010) 3275–3304.

[27] E.J. O'Reilly, T.E. Keyes, R.J. Forster, L. Dennany, Insights into electrochemiluminescent enhancement through electrode surface modification, Analyst 138 (2013) 677–682.

[28] Q. Liu, J. Huan, A.R. Fei, H.P. Mao, K. Wang, "Signal on" electrochemiluminescence pentachlorophenol sensor based on luminol-MWCNTs @graphene oxide nanoribbons system, Talanta 134 (2015) 448–452.

[29] H. Dai, X.P. Wu, H.F. Xu, M.D. Wei, Y.M. Wang, G.N. Chen, Fabrication of a new ECL biosensor for choline by encapsulating choline oxidase into titanate nanotubes and Nafion composite film, Electrochem. Commun. 11 (2009) 1599–1602.

[30] S. Garcia-Segura, F. Centellas, E. Brillas, Unprecedented electrochemiluminescence of luminol on a boron-doped diamond thin-film anode. Enhancement by electrogenerated superoxide radical anion, J. Phys. Chem. C 116 (2012) 15500–15504.

[31] Y.F. Cheng, R. Yuan, Y.Q. Chai, H. Niu, Y.L. Cao, H.J. Liu, L.J. Bai, Y.L. Yuan, Highly sensitive luminol electrochemiluminescence immunosensor based on ZnO nanoparticles and glucose oxidase decorated graphene for cancer biomarker detection, Anal. Chim. Acta 745 (2012) 137–142.

[32] Q. Zhao, S. Tang, Y.F. Tu, Titania nanotubes decorated with gold nanoparticles for electrochemiluminescent biosensing of glycosylated hemoglobin, Anal. Chim. Acta 936 (2016) 83–90.

[33] Z.M. Yu, X.H. Wei, J.L. Yan, Y.F. Tu, Intensification of electrochemiluminescence of luminol on TiO_2 supported Au atomic cluster nano-hybrid modified electrode, Analyst 137 (2012) 1922–1929.

[34] A. Toyota, T. Sagara, Particle size dependence of the charging of Au nanoparticles immobilized on a modified ITO electrode, Electrochim. Acta 53 (2008) 2553–2559.

[35] R.K. Shervedani, S. Pourbeyram, A modification free hybridization biosensor for detection of DNA sequence based on Zr (IV) ion glue mediated the adsorption on Au-MPA SAM electrode, Sensors Actuators B Chem. 160 (2011) 145–153.

[36] S. Deng, L. Cheng, J. Lei, Y. Cheng, Y. Huang, H. Ju, Label-free electrochemiluminescent detection of DNA by hybridization with a molecular beacon to form hemin/G-quadruplex architecture for signal inhibition, Nano 5 (2013) 5435–5441.

[37] G. Li, X. Li, J. Wan, S. Zhang, Dendrimers-based DNA biosensors for highly sensitive electrochemical detection of DNA hybridization using reporter probe DNA modified with Au nanoparticles, Biosens. Bioelectron. 24 (2009) 3281–3287.

[38] G.J. Li, L.H. Liu, X.W. Qi, Y.Q. Guo, W. Sun, X.L. Li, Development of a sensitive electrochemical DNA sensor by 4-aminothiophenol self-assembled on electrodeposited nanogold electrode coupled with Au nanoparticles labeled reporter ssDNA, Electrochim. Acta 63 (2012) 312–317.

[39] S.Y. Zhai, J.L. Yan, Q. Zhao, Y.F. Tu, A label-free genetic biosensor for diabetes based on AuNPs decorated ITO with electrochemiluminescent signaling, Anal. Chim. Acta 982 (2017) 62–71.

[40] A.V. Stoyanov, C.L. Rohlfing, S. Connolly, M.L. Roberts, Use of cation exchange chromatography for human C-peptide isotope dilution-mass spectrometric assay, J. Chromatogr. A 1218 (2011) 9244–9249.

[41] T.C. Liu, M.J. Chen, Z.Q. Ren, J.Y. Hou, G. Feng, L. Ying, S. Wu, Development of an improved time-resolved fluoroimmunoassay for simultaneous quantification of C-peptide and insulin in human serum, Clin. Biochem. 47 (2014) 439–444.

[42] M. Asanghanwa, F. van Genderen, K. Verhaeghen, Validation of an enzyme linked immunosorbent assay for C-peptide analysis in Cameroon, Diabetes Res. Clin. Pract. 98 (2012) 459–464.

[43] M.D. Regulacio, M.H. Pablico, J.A. Vasquez, P.N. Myers, S. Gentry, M. Prushan, Luminescence of LnIII dithiocarbamate complexes (Ln = La, Pr, Sm, Eu, Gd, Tb, Dy), Inorg. Chem. 47 (2008) 1512–1523.

[44] A. Thomas, P.T. Brinkkötter, W. Schänzer, M. Thevis, Simultaneous determination of insulin, DesB30 insulin, proinsulin, and C-peptide in human plasma samples by liquid chromatography coupled to high resolution mass spectrometry, Forensic Toxicol. 35 (2017) 106–113.

[45] M.L. Graham, S.C. Gresch, S.K. Hardy, L.A. Mutch, J.L. Janecek, Evaluation of commercial ELISA and RIA for measuring porcine C-peptide: implications for research, Xenotransplantation 22 (1) (2015) 62–69.

[46] L.M. Wang, N.F. Lovejoy, D.L. Faustman, Persistence of prolonged C-peptide production in Type 1 Diabetes as measured with an ultrasensitive C-peptide assay, Diabetes Care 35 (3) (2012) 465–470.

[47] Q. Ma, L.Q. Li, A. He, G.F. Lin, L.P. Zou, M. Li, Y.S. Wu, Development of the dual-labeling time-resolved fluoroimmunoassay for detection of C-peptide and insulin and its initially application, Prog. Biochem. Biophys. 7 (2011) 670–676.

[48] J. Schultess, C. van Duren, M. Martens, M. Costa, T. Llop, Diagnostic performance of the architect C-Peptide immunoassay, Clin. Chem. Lab. Med. 47 (7) (2009) 834–841.